Extreme Sensitivity of Circular Dichroism to Long-Range Excitonic Couplings in Helical Supramolecular Assemblies

Leon van Dijk,*,† Peter A. Bobbert,† and Frank C. Spano‡

Theory of Polymers and Soft Matter, Department of Applied Physics and Eindhoven Polymer Laboratories, Technische Universiteit Eindhoven, P.O. Box 513, 5600 MB Eindhoven, The Netherlands, and Department of Chemistry, Temple University, Beury Hall 201, Philadelphia, Pennsylvania 19122

Received: November 21, 2009; Revised Manuscript Received: December 3, 2009

Circular dichroism (CD) spectroscopy is an ideal tool for studying the self-assembly of helical supramolecular assemblies since it is very sensitive to extended excitonic couplings between chiral chromophores. We show that the CD spectrum retains its high sensitivity to long-range interactions even in the presence of extreme disorder and strong interaction with vibrations when excitations are mainly localized on individual molecules. We derive a universal expression for the first moment of the CD spectrum of helical assemblies in terms of a modulated sum over excitonic couplings, which is independent of the strength of the energetic disorder, the spatial correlation of the disorder, and the strength of the interaction with vibrations. This demonstrates that excitonic couplings can be directly extracted from experimental CD spectra without having information about the energetic disorder and vibrational interactions. We apply our results to helical assemblies of functionalized chiral oligo(*p*-phenylenevinylene) molecules and show that existing theoretical values for the excitonic couplings should be adapted in order to obtain agreement with the experimental CD spectrum.

1. Introduction

Optical spectroscopy is a very useful tool for obtaining information about the structure of proteins, DNA, liquid crystal phases, and (supra)molecular assemblies.[1−8] These systems have in common that they consist of electronically coupled units, leading to a delocalization of their photoexcitations (excitons). This delocalization affects their optical spectra, and one may therefore attempt to extract the excitonic coupling strength between units using optical spectroscopy. Since this coupling depends on the distance between the units and their relative orientation, optical spectra contain information about the structure of the molecular system under investigation.

Circular dichroism (CD) measures the difference in absorption between left- and right-handed circularly polarized light and is particularly useful for studying molecular systems that involve chiral molecules. Most biological (macro)molecules are chiral, and therefore, CD spectroscopy is widely used to study biological systems.[1−4] For example, CD spectroscopy can be utilized to probe changes in the conformation of biological macromolecules and their interaction with other molecules. More recently, the application of CD spectroscopy has been extended to supramolecular chemistry[7,8] in the study of the supramolecular self-assembly of chiral molecules, which can be used to construct well-organized functional nanomaterials.[9−11]

A beautiful example is the self-assembly of helical MOPV4 aggregates,[12,13] which has received considerable attention lately.[14−23] MOPV4 molecules are chiral oligo(*p*-phenylenevinylene) (OPV) derivatives that are functionalized on one end with a ureidotriazine group; see Figure 1. This end group enables a molecule to engage in four hydrogen bonds with another molecule. H-bonded pairs (dimers) are formed when MOPV4 molecules are dissolved in dodecane solution at high temperature. Upon lowering the temperature, these dimers associate into small randomly ordered aggregates. Below a critical temperature, the randomly ordered assemblies attain a helical conformation, followed by a strong elongation upon further cooling. UV/vis absorption, fluorescence, and CD spectroscopy were used to identify and distinguish different stages in the self-assembly process of helical MOPV4 aggregates as a function of temperature.[13]

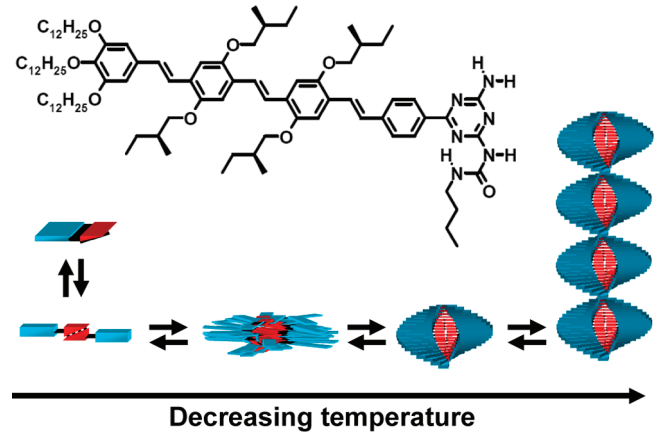

Figure 1. Molecular structure of the monofunctionalized MOPV4 molecule, containing four *p*-phenylenevinylene units, and a schematic representation of the self-assembly. The blue and red blocks represent the OPV4 backbone and the functional H-bonding end group, respectively. Each H-bonded pair of molecules forms a rung of the helix. The distance and pitch angle between two consecutive H-bonded pairs (dimers) along the stacks are $d = 3.75$ Å and about $\phi = 14°$, respectively.[13,20] H-bonded dimers form when MOPV4 molecules are dissolved in dodecane solution at high temperature. Upon lowering the temperature, these dimers associate into small randomly ordered aggregates that transform into long helical assemblies below a critical temperature.

* To whom correspondence should be addressed. E-mail: l.p.v.dijk@tue.nl. Phone: +31 (0)40 247 2438. Fax: +31 (0)40 244 5253

† Technische Universiteit Eindhoven.

‡ Temple University.

10.1021/jp911081b
Published on Web 12/29/2009

The main signature of aggregation of MOPV4 dimers is the appearance of a shoulder on the low-energy side of the absorption spectra,[13,20] whereas the transition into long helices leads to the emergence of a bisignate CD activity (Cotton effect) in the vicinity of the lowest molecular singlet transition, indicative of a left-handed helix.[13,20] Fluorescence spectra of MOPV4 are characterized by a clear vibronic progression due to a symmetric ring breathing/vinyl stretching mode with a frequency of $\sim$1400 cm^{-1}. Upon aggregation, the fluorescence spectra red shift[22] and show a reduction of the 0−0 emission intensity relative to the sideband emission.[20] The absorption, fluorescence, and CD spectral line shapes of the helical MOPV4 aggregates were successfully reproduced in ref 20 by employing the Holstein Hamiltonian with spatially correlated disorder.

Circular dichroism in helical assemblies stems entirely from the excitonic coupling between chiral molecules,[3,4] making this technique very sensitive to this coupling, in contrast to absorption and fluorescence. In fact, it has been known for a long time that the specific signature of a Cotton effect in exciton-coupled dimers can be detected even at very large intermolecular distances.[24−27] For example, in porphyrin dimers covalently bound to an oligonaphthalene scaffold, a Cotton effect was detected at an intermolecular distance as far as 70 Å.[27] More recently, an even more dramatic demonstration of the sensitivity of the CD response to long-range interactions was given in ref 20; limiting the excitonic couplings in a helical MOPV4 aggregate to the first six nearest neighbors (i.e., by setting the seventh and further nearest-neighbor couplings to zero) results in a surprising 30% increase in the CD intensity, whereas there is no discernible effect on the absorption. However, perhaps even more surprising is the fact that this happens while the exciton is localized by energetic disorder to only two MOPV4 molecules. How can the CD response to such localized excitons be so sensitive to long-range excitonic interactions?

In the present work, we study this extreme sensitivity of the CD response to long-range excitonic couplings. Our analysis starts in section 2 with a study of CD in helical assemblies without interactions between excitations and vibrations (exciton−phonon interaction). Harada and co-workers showed that the magnitude of the CD response in disorder-free assemblies is directly related to a sum over all extended excitonic couplings.[24] We will show that the magnitude of the CD response in the presence of energetic disorder decreases with increasing disorder strength but that this magnitude is still proportional to exactly the same sum. This leads to the surprising conclusion that the sensitivity of CD to extended excitonic couplings is unaffected by disorder; even very strong localization of the exciton does not affect this sensitivity. Another important quantity characterizing the CD spectrum is its first spectral moment. This quantity is unaffected by energetic disorder and also proportional to the above sum over all extended excitonic couplings, as has been shown by Somsen et al.[28] and Burin et al.[29] Burin and co-workers neglected further than nearest-neighbor couplings in their analysis of exciton couplings in DNA hairpins.[29] This is justified due to the relatively large angle between the base pairs comprising the DNA hairpins ($\sim$36°). We will show that long-range excitonic couplings can actually have a significant contribution in helical aggregates with smaller pitch angles, and we will show that the CD first spectral moment is very sensitive to these long-range couplings.

In section 3, we will consider the realistic case of the presence of exciton−phonon interaction and spatially correlated energetic disorder. We will show that the relation between the first CD spectral moment and the sum over all extended excitonic couplings is unaffected by the exciton−phonon interaction and the spatial correlation of the energetic disorder. This leads to the important conclusion that CD spectroscopy is indeed a very useful experimental tool for probing extended couplings since information about these couplings can be extracted without the need to have information about the energetic disorder and the exciton−phonon interaction. We apply our results to the MOPV4 helices and show that while inclusion of both correlated energetic disorder and exciton−phonon interaction is essential to describe the absorption and luminescence spectra,[20] it has no influence at all on the sensitivity of the CD spectrum to long-range excitonic couplings. In section 4, we give a summary of our results and our main conclusions and propose a method to extract excitonic couplings using CD spectroscopy on templated assemblies.

2. Helical Assemblies with Energetic Disorder

In this section, we study CD in helical assemblies with spatially uncorrelated energetic disorder without exciton−phonon interaction. We model the helical assemblies as linear chains consisting of N two-level chromophores with radially oriented transition dipoles. The exciton Hamiltonian of the system is given by

$$H = \omega_{0-0} + D + \sum_{n}^{N} \Delta_n |n\rangle\langle n| + \sum_{n=1}^{N} \sum_{m \neq n} J_{nm} |n\rangle\langle m| \tag{1}$$

where we have set $\hbar = 1$ and where $|n\rangle$ denotes an electronic state in which chromophore n is electronically excited while all other chromophores remain in the electronic ground state. The energy needed for exciting a chromophore from its electronic ground state to its first optically allowed excited state is the transition energy. For the nth chromophore, the transition energy is given by $\omega_{0-0} + D + \Delta_n$, where ω_{0-0} is the gas-phase 0−0 transition energy and D is the gas-to-crystal shift due to nonresonant interactions. The randomly assigned transition energy offsets Δ_n account for fluctuations in transition energies along the aggregates. These transition energies fluctuate due to thermally induced deformations within each chromophore (e.g., by bending and twisting) or due to randomness in the direct environment of the chromophores because of the presence of solvent molecules. To model the effect of this energetic disorder, we draw the transition energy offsets Δ_n from a Gaussian distribution function with standard deviation σ. The off-diagonal elements of H account for the exciton coupling between the nth and mth chromophores. We will study the case of dipole−dipole coupling, for which $J_{nm} = J \cos[(n - m)\phi]/|n - m|^3$, with $J > 0$ as the excitonic coupling between nearest neighbors and ϕ as the pitch angle between the radially oriented transition dipole moments of consecutive chromophores. Because of the finite size of the molecules, however, excitonic couplings can often not be described by a simple dipole−dipole coupling. Therefore, we will also study the case of the excitonic couplings between chromophores in MOPV4 aggregates. These exciton couplings were obtained from ref 20, and they have been evaluated by combining a coupled cluster single and double (CCSD) approach to the INDO Hamiltonian on the basis of model geometric structures; see ref 15.

In what follows, we evaluate the absorption spectrum, $A(\omega)$, and the circular dichroism spectrum, CD(ω), for a helical assembly using the expressions

$$A(\omega) = \langle \sum_{\alpha} d_{\alpha} \Gamma(\omega - \omega_{\alpha}(C)) \rangle_{C} \quad (2)$$

and

$$\mathrm{CD}(\omega) = \langle \sum_{\alpha} R_{\alpha} \Gamma(\omega - \omega_{\alpha}(C)) \rangle_{C} \quad (3)$$

respectively. Here $\langle ... \rangle_C$ denotes an average over disorder configurations, and $\Gamma(\omega - \omega_\alpha)$ is a symmetric line shape function centered about the energy of the αth eigenstate ω_α of the exciton Hamiltonian. For this line shape function, we use a Gaussian, with its standard deviation σ_H representing the homogeneous line width and its integral normalized to 1. Throughout the paper, we use $\sigma_H = 14$ meV for calculating absorption and CD spectra. This value is small enough for all cases studied to guarantee that the spectral broadening is dominated by the energetic disorder but large enough to obtain smooth spectra. For consistency, we will use the same value in our analysis of disorder-free helical aggregates. The dimensionless absorption and rotational line strengths in eqs 2 and 3 are given by

$$d_{\alpha} = \frac{1}{\mu^2} \left| \sum_{n} \langle \psi^{(\alpha)} | \hat{\mu}_n | G \rangle \right|^2 \quad (4)$$

and[3,4]

$$R_{\alpha} = \frac{k_{\lambda}}{\mu^2} \sum_{n} \sum_{n'} \langle \psi^{(\alpha)} | \hat{\mu}_n | G \rangle \times \langle G | \hat{\mu}_{n'} | \psi^{(\alpha)} \rangle \cdot (\mathbf{r}_n - \mathbf{r}_{n'}) \quad (5)$$

Here, $|\psi^{(\alpha)}\rangle \equiv \sum_n c_n^{(\alpha)} |n\rangle$ is the wave function of the αth eigenstate (the coefficients $c_n^{(\alpha)}$ can be chosen to be real), and $|G\rangle$ is the ground state of the assembly in which all molecules are in their electronic ground state $|g\rangle$. In addition, $k_\lambda \equiv \omega_{0-0}/c$, with c as the speed of light, μ as the transition dipole moment (tdm) of the individual chromophores, and $\hat{\mu}_n$ as the molecular tdm operator. With the helical axis directed along the z-axis, the tdm operator of the nth chromophore is

$$\hat{\mu}_n = \mu(\cos(n\phi)\hat{e}_x - \sin(n\phi)\hat{e}_y)|n\rangle\langle g| + \mathrm{H.c.} \quad (6)$$

with $\hat{e}_x$ and $\hat{e}_y$ as the unit vectors in the x and y directions. This definition of the tdm operator corresponds to a left-handed (right-handed) helix for $\phi > 0$ ($\phi < 0$). Inserting the wave function of the αth eigenstate into eqs 4 and 5 leads to expressions for the line strengths in terms of the wave function coefficients $c_n^{(\alpha)}$

$$d_{\alpha} = \sum_{n} \sum_{m} c_n^{(\alpha)} c_m^{(\alpha)} \cos[(n - m)\phi] \quad (7)$$

and

$$R_{\alpha} = k_{\lambda} d \sum_{n} \sum_{m} c_n^{(\alpha)} c_m^{(\alpha)} (n - m) \sin[(n - m)\phi] \quad (8)$$

Figure 2 shows absorption (dotted lines) and CD (solid lines) spectra of a helical assembly containing $N = 30$ chromophores with pitch angle of $\phi = 14°$ and with the calculated excitonic couplings from ref 20. This results in an exciton bandwidth of $W = 150$ meV, with the exciton bandwidth W defined as the energy difference between the highest-energy and lowest-energy exciton states when energetic disorder is absent. Figure 2 shows spectra of disorder-free assemblies (a) and assemblies with strong energetic disorder (b) for the inclusions of all excitonic couplings (black lines) and for excitonic couplings truncated after $N_{tr} = 1$ (red lines), 6 (green lines), and 12 (blue lines) nearest neighbors. In general, the absorption spectra are blue-shifted, which is characteristic for H-aggregates ($J > 0$), and the corresponding CD spectra for the left-handed helix show the classic bisignate Cotton effect and cross zero at the peak of the absorption spectrum.

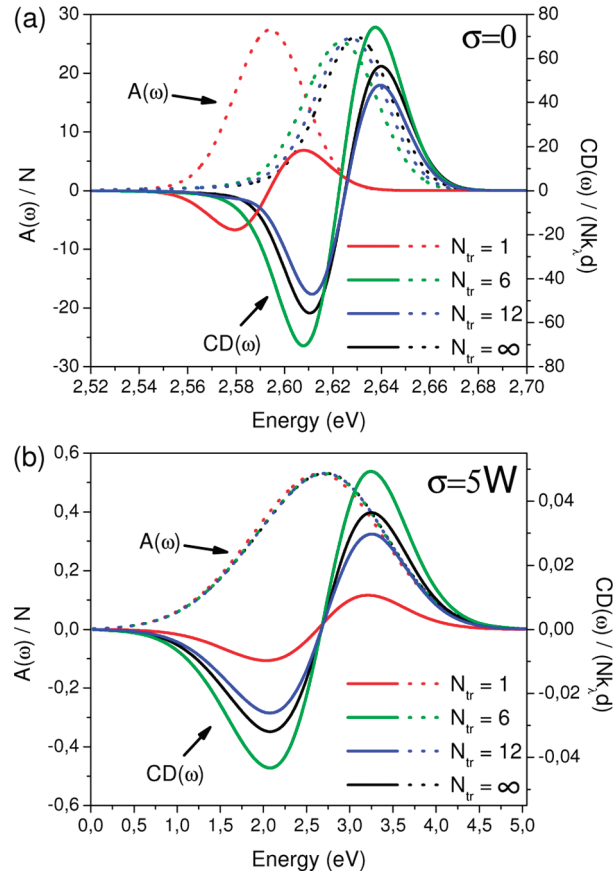

Figure 2. Calculated absorption (dotted lines) and CD (solid lines) spectra of a helical assembly containing $N = 30$ chromophores with a pitch angle of $\phi = 14°$ for the calculated excitonic couplings of ref 20, leading to an exciton bandwidth of $W = 150$ meV for a disorder-free assembly. The homogeneous line width is set to $\sigma_H = 14$ meV, and the average chromophore transition energy is $\omega_{0-0} + D = 2.53$ eV. Spectra are shown for (a) disorder-free assemblies and (b) assemblies with strong disorder $\sigma = 5W$, with inclusion of all excitonic couplings and with excitonic couplings truncated after N_{tr} nearest neighbors. Note the different x - and y-scales in (a) and (b).

Figure 2 demonstrates that the magnitude of the CD response is very sensitive to extended excitonic couplings. With respect to the spectrum with all couplings included, truncating the extended excitonic coupling beyond $N_{tr} = 1$ and 12 nearest neighbors results in a decrease of the CD intensity of about 70 and 20%, respectively, whereas truncating beyond $N_{tr} = 6$ nearest neighbors leads to an increase of about 35%. Amazingly, the magnitude of the CD response in assemblies with strong energetic disorder is just as sensitive to extended excitonic couplings as it is for disorder-free assemblies, despite the fact that strong localization of the excitonic states has taken place.

In contrast to the CD spectra, the absorption spectra are far less sensitive to extended excitonic couplings. The absorption spectra of assemblies with strong energetic disorder are practically identical, while for disorder-free assemblies, differences in the blue shift of the spectra are discernible, especially for the $N_{tr} = 1$ spectrum, which has a smaller blue shift than the other absorption spectra.

For sufficiently long disorder-free assemblies, the only optically allowed states are the degenerate exciton states with wave vectors $k = \pm\pi\phi/180$, with ϕ expressed in degrees.[30,31] The absorption spectrum is then very accurately described by

$$A(\omega)/N = \Gamma(\omega - \omega_{0-0} - D - J_\phi) \tag{9}$$

Here, J_ϕ is the spectral blue shift given by

$$J_\phi = \frac{2}{N}\sum_{n=1}^{N}\sum_{s>0} J_{n,n+s}\cos(s\phi) \tag{10}$$

which is the excitonic contribution to the energy of the optically allowed degenerate exciton states with wave vectors $k = \pm\pi\phi/180$. These excitonic states are also the only states that contribute significantly to the CD spectrum. In that case, we can derive an expression for the CD spectrum by using a procedure similar to that employed by Harada and co-workers,[24] in which the Gaussian distribution function appearing in eq 3 is Taylor-expanded in the small deviations $(\omega_\alpha - J_\phi)/\sigma_H$. Using this procedure,[6] we find

$$\mathrm{CD}(\omega) = 2k_\lambda d\{\sum_n\sum_{s>0} J_{n,n+s}s\sin(s\phi)\}\frac{\omega - \omega_{0-0} - D - J_\phi}{\sigma_H^2} \times \Gamma(\omega - \omega_{0-0} - D - J_\phi) \tag{11}$$

We numerically checked that eqs 9 and 11 describe the absorption and CD spectra for disorder-free assemblies very accurately if the assemblies are sufficiently long ($N > 100$). We note that eq 11 agrees with the expression derived by Didraga and co-workers[31] for the special case of radially directed transition dipole moments.

A good measure for the magnitude of the CD response is the absolute value of the difference between the CD maximum and minimum, $|A_{CD}|$. For disorder-free assemblies, it follows from eq 11 that

$$|A_{CD}| = \frac{4k_\lambda d}{\sqrt{2\pi e}\sigma_H^2}\sum_n\sum_{s>0} J_{n,n+s}s\sin(s\phi) \tag{12}$$

As is clear from this expression, $|A_{CD}|$ is proportional to an $s\sin(s\phi)$-modulated sum over couplings, which is responsible for the extreme sensitivity of CD to extended excitonic couplings. This is illustrated in Figure 3, which shows the calculated excitonic couplings $J_{n,n+s}$ for MOPV4 aggregates[20] as a function of s, together with the cosine-modulated couplings (inset: red circles) and the much longer range $s\sin(s\phi)$-modulated couplings (inset: blue triangles). Figure 3 clearly demonstrates that the $s\sin(s\phi)$-modulated interaction sum that appears in eqs 11 and 12 is much more sensitive to extended interactions than the cosine-modulated sum J_ϕ that causes the spectral shift of the absorption spectrum. This makes CD spectroscopy particularly sensitive to long-range interactions, as was first pointed out by Harada and co-workers[24] and later by others.[25−27]

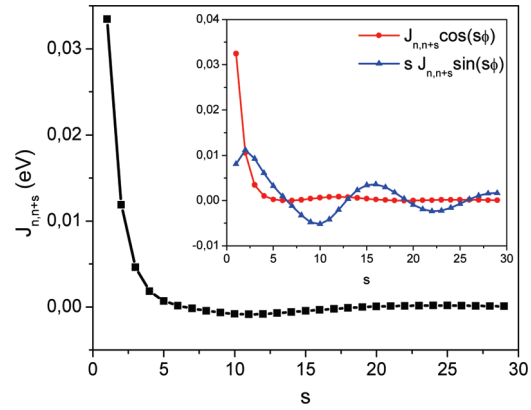

Figure 3. Calculated excitonic couplings $J_{n,n+s}$ from ref 20 for MOPV4 aggregates as a function of the intermolecular distance s in units of the lattice constant d. Shown in the inset are the cosine-modulated interactions responsible for the spectral shift of the absorption (red circles) and the much longer range $s\sin(s\phi)$-modulated interactions responsible for the strength of the CD response (blue triangles).

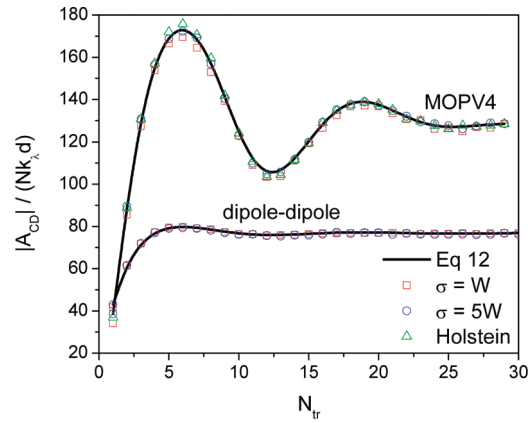

Figure 4. Magnitude of the CD response $|A_{CD}|$ as a function of N_{tr} for a helical assembly with a pitch angle of $\phi = 14°$ for the case of excitonic couplings as calculated in ref 20 for MOPV4 ($N = 30$ chromophores) as well as for dipole−dipole excitonic couplings ($N = 100$). The solid lines correspond to eq 12 for the disorder-free case and a homogeneous line width $\sigma_H = 14$ meV. The symbols represent $|A_{CD}|$ as determined from numerically obtained spectra, normalized to match eq 12 at $N_{tr} = 30$, for $\sigma = W$ (red squares) and $5W$ (blue circles). The green triangles correspond to the normalized $|A_{CD}|$ obtained with the disordered Holstein model in section 3, with spatially correlated disorder, and with aggregate parameters $\omega_{0-0} + D = 2.53$ eV, $\sigma = 85$ meV, $l_0 = 4.5$, $\omega_0 = 0.172$ eV, and $\lambda^2 = 1.2$.

For disorder-free assemblies, the sensitivity to extended excitonic couplings is interesting but perhaps not so surprising because the excitonic states are delocalized over the entire assembly. Energetic disorder has a localizing effect on excitations, and one would expect that CD spectra become less sensitive to extended interactions with increasing disorder. However, Figure 2 shows that the CD spectrum is just as sensitive to extended excitonic couplings in the case of strong energetic disorder. This is illustrated further in Figure 4, which shows $|A_{CD}|$ as a function of the truncation distance N_{tr} for an MOPV4 helix consisting of $N = 30$ chromophores and a pitch angle of $\phi = 14°$. We have also calculated $|A_{CD}|$ for a helix consisting of $N = 100$ chromophores with dipole−dipole coupling $J_{nm} = J\cos[(n - m)\phi]/|n - m|^3$ and the same pitch

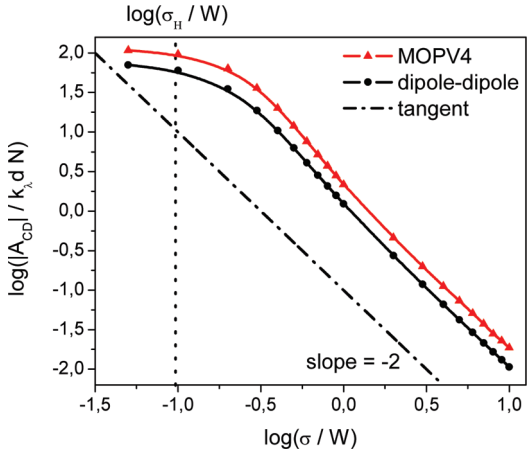

Figure 5. Magnitude of the CD response $|A_{CD}|$ versus the ratio of the disorder strength and the exciton bandwidth, σ/W, for the case of excitonic couplings calculated for MOPV4 in ref 20 as well as for the case of dipole−dipole excitonic couplings. If the inhomogeneous broadening σ is much larger than the homogeneous broadening σ_H, $|A_{CD}|$ is proportional to σ^{-2}, as indicated by the dash−dotted line.

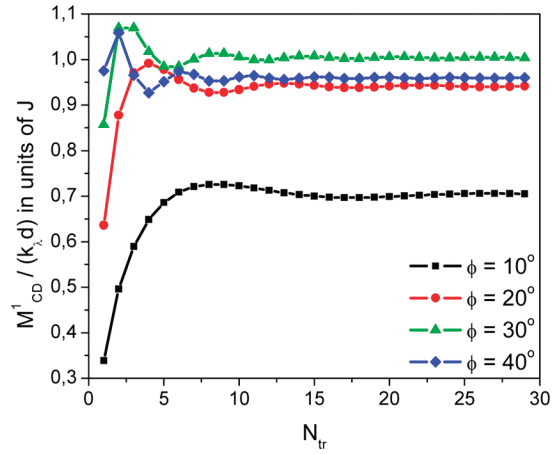

Figure 6. First spectral moment M^1_{CD} of the CD spectrum as a function of N_{tr} for the dipole−dipole interaction and $N = 100$ chromophores. Results are shown for different pitch angles.

angle. The nearest-neighbor coupling was set to $J = 38$ meV, leading to a disorder-free bandwidth of $W = 150$ meV, equal to that of a disorder-free MOPV4 helix. The solid lines in Figure 4 represent eq 12, which gives $|A_{CD}|$ for disorder-free assemblies, whereas the symbols correspond to $|A_{CD}|$ for $\sigma = W$ (red squares) and $5W$ (blue circles), determined from numerically obtained spectra and normalized to match eq 12 at $N_{tr} = 30$. For both disorder strengths, we find that $|A_{CD}|$ remains proportional to the $s\sin(s\phi)$-modulated interaction sum present in eq 12 and therefore remains highly sensitive to extended interactions, even in the presence of strong energetic disorder.

Although energetic disorder does not affect the extreme sensitivity of CD to extended excitonic couplings, it certainly has a dramatic effect on the magnitude of the CD response. Figure 2 shows that the CD maximum decreases by a factor of 1500 if the energetic disorder strength is increased from $\sigma = 0$ to $5W$. To illustrate this further, we show in Figure 5 $|A_{CD}|$ as a function of the ratio σ/W of the inhomogeneous line width and the disorder-free exciton bandwidth. As indicated by the dash−dotted line, $|A_{CD}|$ is proportional to σ^{-2} as long as the inhomogeneous broadening σ is much larger than the homogeneous broadening σ_H. Figure 5 demonstrates that strong localization of the exciton due to energetic disorder causes a significant decrease in the magnitude of the CD response.

A very useful quantity to characterize the CD spectrum is its first spectral moment, which we define as

$$M^1_{CD} \equiv \frac{\int_0^\infty \omega \mathrm{CD}(\omega)\mathrm{d}\omega}{\int_0^\infty A(\omega)\mathrm{d}\omega} \tag{13}$$

Experimentally, normalization by the total absorption is convenient because this makes M^1_{CD} an intensive quantity that does not depend on the magnitude of the transition dipole moments and the optical path length. Theoretically, we have $\int A(\omega)\mathrm{d}\omega = N$. Somsen et al.[28] and Burin et al.[29] derived for the case at hand expressions for M^1_{CD} that can be written as

$$M^1_{CD} = \frac{2k_\lambda d}{N}\sum_n \sum_{s>0} J_{n,n+s} s \sin(s\phi) \tag{14}$$

Equation 14 shows that M^1_{CD} depends only on an $s\sin(s\phi)$-modulated sum of couplings and not on the strength of the energetic disorder. Figure 6 shows M^1_{CD} as a function of the truncation distance N_{tr} for the case of dipole−dipole coupling and with different pitch angles. We checked eq 14 against the first spectral moment obtained from numerically calculated CD spectra and found perfect agreement. Figure 6 demonstrates that M^1_{CD} is quite sensitive to N_{tr}, making it a very useful quantity for probing long-range excitonic interactions.

In ref 29, Burin et al. used the experimentally determined CD first spectral moment to extract the exciton coupling between AT−AT and AT−TA base pairs in DNA hairpins, and they found good agreement with the numerically calculated value. They assumed that the contribution of further than nearest-neighbor couplings are negligible. Our results clearly show that these couplings can actually have a significant contribution. However, the angle between the AT base pairs in the DNA hairpins studied in ref 29 is about 36°. Figure 6 demonstrates that the CD first spectral moment is far less sensitive to further than nearest-neighbor interactions if the pitch angle is around 40°. Therefore, for this specific case, no significant error is made if further than nearest-neighbor interactions are neglected. In general, however, long-range couplings will have to be taken into account.

The consideration of the first spectral moment also provides an explanation for the proportionalities to σ^{-2} and the $s\sin(s\phi)$-modulated interaction sum of the magnitude $|A_{CD}|$ of the CD spectrum. In the strong-disorder limit, the CD spectral line shape is quite accurately described by the function $C(\omega - \omega_{0-0} - D)\exp[-(\omega - \omega_{0-0} - D)^2/2\sigma^2]$, where the constant C determines the magnitude of the CD response. Since the relation $\int\omega\mathrm{CD}(\omega)\mathrm{d}\omega = NM^1_{CD}$ should be obeyed for any disorder strength, we find that $C \propto M^1_{CD}\sigma^{-2}$, and hence, $|A_{CD}|$ is proportional to σ^{-2} and to the $s\sin(s\phi)$-modulated interaction sum.

We obtain further understanding of this result by considering the strong-disorder limit. Excitonic coupling then acts as a perturbation, and we can apply perturbation theory to find the rotational line strengths. This procedure was followed in ref 4 for the case of an exciton-coupled dimer. We have extended this approach to helical N-mers, for which we refer to the Supporting Information. The final result for the rotational line strength of the αth eigenstate, which is strongly localized to the αth chromophore, is

$$R_\alpha \approx -k_\lambda d \sum_{n\neq\alpha} \frac{J_{n\alpha}}{2(\Delta_n - \Delta_\alpha)}(n-\alpha)\sin[(n-\alpha)\phi] \tag{15}$$

which should be inserted into eq 3 to obtain the CD spectrum. In the average over all disorder configurations, each term in eq 15 becomes proportional to $\langle 1/(\Delta_n - \Delta_\alpha)\rangle_C$, which is independent of the distance between the nth and αth chromophore, $(n - \alpha)$. The rotational line strength is therefore proportional to the s $\sin(s\phi)$-modulated sum over all exciton couplings. Furthermore, on average, the energy difference $\Delta_n - \Delta_\alpha$ is on the order of σ, leading to a scaling of the rotational line strengths with σ^{-1}. Since, in addition, inhomogeneous broadening spreads the absorption of light over an energy range that scales with σ, the CD intensity becomes indeed proportional to σ^{-2}.

3. Helical Assemblies with Exciton−Phonon Interaction and Correlated Disorder

In this section, we study the dependence of CD on extended excitonic couplings in the presence of spatially correlated disorder and exciton−phonon interaction, which are both important in describing realistic systems. Organic materials, such as MOPV4 helices, are soft in the sense that the electronic excitations are accompanied by significant nuclear rearrangements in the participating chromophores. In comparison with the model discussed in the previous section, the photophysics of MOPV4 helices is therefore much more complicated. We will investigate how the interaction of excitons with intermolecular vibrations (exciton−phonon interaction) affects the findings of the previous section.

The general model used to account for the photophysics of MOPV4 helices is the disordered Holstein model,[32] which was introduced in ref 20. We limit ourselves here to a brief summary of the model, and we refer to ref 20 for a detailed discussion. In short, the disordered Holstein Hamiltonian includes excitonic coupling between chromophores (MOPV4 molecules), exciton−phonon interaction, and disorder in the transition energies. The MOPV4 helices are modeled as a linear chain of N two-level chromophores with an electronic ground state $|g\rangle$ and an energetically lowest-lying excited state $|e\rangle$. For the nth chromophore, the transition energy is $\omega_{0-0} + D + \Delta_n$. As in ref 20, we assume spatially correlated disorder and the covariance between two randomly assigned transition energy offsets Δ_n and Δ_m is given by $\langle \Delta_n \Delta_m\rangle_C = \sigma^2 \exp(-|n-m|/l_0)$. Here, σ is again the standard deviation of the Gaussian distribution function representing the disorder strength, and l_0 is the spatial correlation length in dimensionless units of the lattice spacing. This form was originally used by Knapp in a study of the line shapes of J aggregates.[33] In ref 20, a good agreement with the experimental spectra was obtained with $\omega_{0-0} + D = 2.53$ eV, $\sigma = 85$ meV, and $l_0 = 4.5$, and we adopt these values here.

The exciton−phonon coupling arises from coupling of each MOPV4 chromophore to a high-energy intramolecular symmetric ring breathing/vinyl stretching vibrational mode with frequency $\omega_0 = 0.172$ eV (1400 cm^{-1}) and Huang−Rhys factor λ^2. The Huang−Rhys factor is a measure for the shift in the equilibrium configuration of the ground- and excited-state nuclear arrangements. We use a Huang−Rhys factor of $\lambda^2 = 1.2$. This value, together with the cubic frequency dependence of the emission rate, yields roughly equal single-molecule 0−0 and 0−1 emission peak intensities, as is found for OPV4 molecules in solution.[34] This vibrational mode is responsible for the formation of polaronic excitons, which are also called neutral polarons.

To represent the eigenstates of the disordered Holstein Hamiltonian, we use the two-particle approximation.[35,36] Within this approximation, the αth eigenstate of the Hamiltonian is given by

$$|\psi^{(\alpha)}\rangle = \sum_{n,\tilde{\nu}} c^{(\alpha)}_{n,\tilde{\nu}} |n,\tilde{\nu}\rangle + \sum_{n,\tilde{\nu}}\sum_{n',\nu'} c^{(\alpha)}_{n,\tilde{\nu};n',\nu'} |n,\tilde{\nu};n',\nu'\rangle \tag{16}$$

where the coefficients $c^{(\alpha)}_{n,\tilde{\nu}}$ and $c^{(\alpha)}_{n,\tilde{\nu};n',\nu'}$ can be chosen to be real. The first term of this expansion represents the one-particle states. A one-particle state $|n,\tilde{\nu}\rangle$ consists of a vibronic (both electronic and vibrational) excitation at chromophore n containing $\tilde{\nu}$ vibrational quanta in the shifted excited-state nuclear potential. All other chromophores remain electronically and vibrationally unexcited. The second term represents the two-particle states. In addition to a vibronic excitation at chromophore n, a two-particle state $|n,\tilde{\nu};n',\nu'\rangle$ has a vibrational excitation at chromophore n' containing ν' vibrational quanta in the ground-state nuclear potential ($\nu' \geq 1$). Inserting the wave function of the αth eigenstate into eqs 4 and 5 leads to expressions for the line strengths in terms of the multiparticle coefficients

$$d_\alpha = \sum_{n,n'}\sum_{\tilde{\nu},\tilde{\nu}'} c^{(\alpha)}_{n,\tilde{\nu}} c^{(\alpha)}_{n',\tilde{\nu}'} f_{\tilde{\nu}0} f_{\tilde{\nu}'0} \cos[(n-n')\phi] \tag{17}$$

and

$$R_\alpha = k_\lambda d \sum_{n,n'}\sum_{\tilde{\nu},\tilde{\nu}'} c^{(\alpha)}_{n,\tilde{\nu}} c^{(\alpha)}_{n',\tilde{\nu}'} f_{\tilde{\nu}0} f_{\tilde{\nu}'0} (n-n')\sin[(n-n')\phi] \tag{18}$$

Here, $f_{\tilde{\nu}\nu} \equiv \langle \tilde{\nu}|\nu\rangle$ is the overlap between the harmonic oscillator eigenfunction with $\tilde{\nu}$ vibrational quanta in the shifted excited nuclear potential and the eigenfunction with ν vibrational quanta in the ground-state nuclear potential. Equations 17 and 18 show that one-particle coefficients contribute directly to the line strengths. Two-particle coefficients contribute only indirectly through normalization of the wave function. The contribution of two-particle states is more evident in emission, enabling the evaluation of the polaron radius from the circularly polarized emission.[20]

Remarkably, it turns out that the expression eq 14 for the CD first spectral moment is also valid for the disordered Holstein Hamiltonian with any type of spatial correlation of the disorder. The proof of this result can be found in the Supporting Information, and it generalizes the results of Somsen et al.[28] and Burin et al.[29] to include exciton−phonon interaction. We thus come to the important conclusion that the first spectral moment of the CD spectrum is unaffected by the inclusion of both correlated energetic disorder and exciton−phonon interaction and depends only on excitonic couplings. Indeed, we find perfect agreement between the first spectral moment obtained from our calculations and eq 14. The normalized magnitude of the CD response $|A_{CD}|$ as a function of N_{tr} is included in Figure 4 of the previous section (green triangles) and falls on top of the results obtained without inclusion of exciton−phonon interaction and spatial correlation of the energetic disorder. These results show that for realistic systems, including exciton−phonon interaction and spatially correlated disorder, the CD spectrum is a very accurate probe of long-range excitonic couplings and that information about these couplings can be

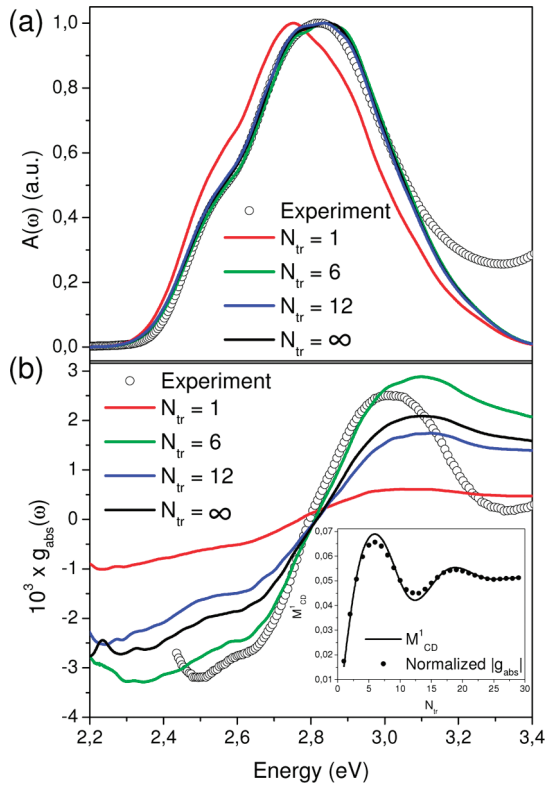

Figure 7. Symbols: experimental absorption (a) and absorption dissymmetry (b) versus energy for MOPV4 aggregates formed in dodecane solution at $T = 278$ K (black dots, from ref 20). Solid black lines: theoretical prediction, based on the exciton couplings from ref 20, for aggregates consisting of $N = 30$ chromophores. The aggregate parameters are $\omega_{0-0} + D = 2.53$ eV, $\sigma = 85$ meV, $l_0 = 4.5$, $\omega_0 = 0.172$ eV, and $\lambda^2 = 1.2$. Red, green, and blue lines: excitonic couplings truncated beyond $N_{tr} = 1$, 6, and 12 units, respectively. Inset: first spectral moment M^1_{CD} (solid line) and the normalized difference between the the maximum and minimum of $g_{abs}(\omega)$ (symbols) as a function of truncation distance N_{tr} for $N = 30$. The latter is normalized to match M^1_{CD} at $N_{tr} = 30$.

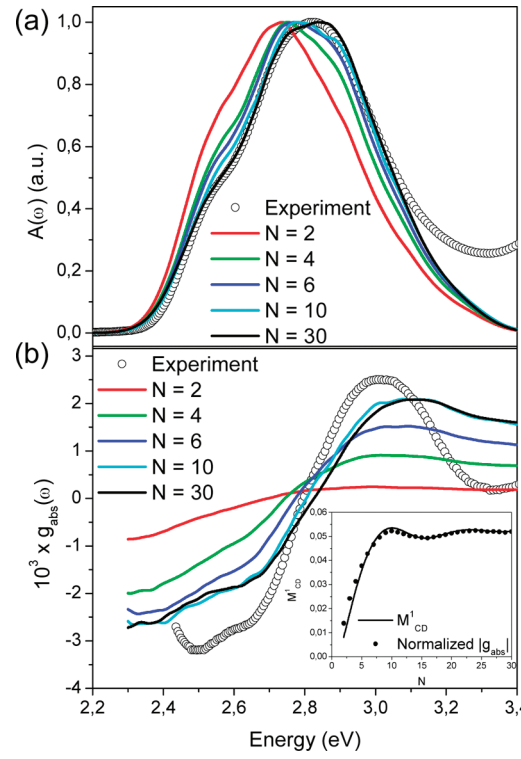

Figure 8. The same as in Figure 7, but now, the dependence on aggregate lengths N is investigated, taking into account all excitonic couplings, $N_{tr} = \infty$. The black lines are identical to the black lines in Figure 7. Inset: first spectral moment M^1_{CD} and the normalized difference between the maximum and minimum of $g_{abs}(\omega)$ as a function of aggregate length N for $N_{tr} = \infty$. The latter is normalized to match M^1_{CD} at $N = 30$.

extracted without having information about the exciton-phonon coupling strength and the strength and type of disorder. Of course, CD does not yield unique information on couplings and therefore the structure of complex assemblies of chromophores cannot uniquely be determined from the CD spectrum.

Figure 7 shows the experimental absorption (a) and absorption dissymmetry (b), $g_{abs}(\omega) \equiv CD(\omega)/A(\omega)$, for MOPV4 helices formed in solution at $T = 278$ K, as compared to theoretical predictions, based on the excitonic couplings of ref 20. In contrast to the CD spectrum, $g_{abs}(\omega)$ is an intensive quantity that does not depend on the magnitude of the transition dipole moment and the optical path length. It represents the net degree of circular polarization normalized to the total absorption. In ref 20, it was reported that the calculated $A(\omega)$ and $g_{abs}(\omega)$ including all excitonic couplings (black solid lines) reproduce the experimental line shapes quite well but that the magnitude of $g_{abs}(\omega)$ is about 30% smaller in comparison to experiment. The best result for $g_{abs}(\omega)$ was obtained for a truncation distance of $N_{tr} = 6$ units,[20] which is shown in Figure 7 as well (green line). We note that the excitonic couplings of ref 20 have been calculated without accounting for dielectric screening effects. Such effects are expected to reduce the excitonic couplings at large distance, which could explain the fact that the best agreement was obtained by omitting couplings beyond $N_{tr} = 6$.

We have also displayed in Figure 7 the results for a truncation distance of the coupling of $N_{tr} = 1$ (red line) and 12 (blue line). Clearly, N_{tr} has a considerable influence on $g_{abs}(\omega)$. On the other hand, apart from $N_{tr} = 1$, the truncation distance has virtually no influence on the absorption spectrum. Figure 7b shows that the worst agreement with the experimental CD spectrum is obtained if only nearest-neighbor couplings ($N_{tr} = 1$) are included. This result demonstrates the importance of extended excitonic couplings for CD. Furthermore, for $N_{tr} = 6$, the magnitude of $g_{abs}(\omega)$ increases by 30% with respect to the results for $N_{tr} = \infty$, whereas in going from $N_{tr} = 6$ to 12, the magnitude of $g_{abs}(\omega)$ drops by about 40%. In fact, the inset of Figure 7b shows that the difference between the maximum and the minimum of $g_{abs}(\omega)$ has essentially the same dependence on truncation distance N_{tr} as the CD first spectral moment M^1_{CD}. The present analysis demonstrates that our results can be used to judge predictions for the exciton couplings, which are intimately related to the structure of the helical assemblies and to dielectric screening effects.

Since the CD first spectral moment M^1_{CD} and magnitude scale with the $s \sin(s\phi)$-modulated interaction sum, they depend also on the number of chromophores in the helical assembly. We display in Figure 8 the absorption (a) and absorption dissymmetry (b) for aggregates of different lengths N. The aggregate length clearly has a considerable influence on $g_{abs}(\omega)$, whereas the absorption spectra for $N = 6$ and 10 have nearly converged to the $N = 30$ spectrum. The slow convergence of the CD spectrum with size in comparison to the absorption spectra was also found by Didraga et al. in their analysis of helical cylindrical assemblies.[31,37] The inset of Figure 8b shows how M^1_{CD} changes as a function of aggregate length N. The largest change of M^1_{CD} occurs between 2 and 10 chromophores, while M^1_{CD} has converged for about 20 or more chromophores. These results

are of importance for the analysis of the aggregation process of helices by measuring the CD activity. For aggregation with a high degree of cooperativity, the growth of the assembly is very rapid, so that one can safely assume that in the analysis of CD spectra, N is very large. This is the case for the self-assembly of MOPV4 aggregates.[13] However, in the case of noncooperative, isodesmic aggregation, the growth of the assemblies is more gradual, and short assemblies will coexist with longer assemblies. In that case, taking into account the dependence of the CD activity on the assembly length becomes crucial in the analysis of CD spectra.

4. Summary, Conclusions, and Outlook

We have studied circular dichroism (CD) in supramolecular helical assemblies with long-range excitonic couplings, with and without energetic disorder, spatial correlation of this disorder, and exciton−phonon interaction. We have found that the magnitude of the CD response and the first moment of the CD spectrum are extremely sensitive to extended excitonic couplings, such that even for the fast decaying dipole−dipole coupling, the CD intensity has only converged after including the 10th nearest-neighbor coupling. We have derived an expression for the first CD spectral moment in terms of a modulated sum over extended excitonic couplings, which is unaffected by energetic disorder, spatial correlation of this disorder, and exciton−phonon interaction. This leads to the remarkable conclusion that information about excitonic couplings can be extracted from experimental CD spectra without the need to have information about the energetic disorder and the exciton−phonon interaction.

We have studied absorption and CD spectra of helical MOPV4 aggregates using the disordered Holstein Hamiltonian with correlated disorder and excitonic couplings calculated with quantum chemical techniques.[20] Long-range excitonic couplings have almost no influence on the absorption spectrum but change the CD spectrum dramatically. Including only nearest-neighbor couplings leads to a CD activity that is a factor of four too small as compared to experiment, while taking into account couplings up to the sixth nearest neighbor leads to good agreement. With the results of the present work, we can fully rationalize this extreme sensitivity to long-range excitonic couplings. Including all extended couplings leads to a CD activity that is about 30% too low, which we attribute to the absence of dielectric screening effects in the quantum chemical calculations. This demonstrates how the results of the present work can be used in judging predictions for excitonic couplings, giving insight into the structure of the helical assemblies and into dielectric screening effects.

Due to the extreme sensitivity to extended excitonic couplings, the assembly length also sensitively affects the CD spectrum. For example, the CD first spectral moment of MOPV4 aggregates increases by more than a factor of 5 if the aggregate length is increased from 2 to 10 chromophores. This property can be very useful to extract extended excitonic couplings from experiment if one can accurately control the length of the helical assemblies. One of the most promising methods for creating helical N-mers with well-defined length N employs single-stranded DNA (ss-DNA) as a template for naphthalene- and oligophenylenevinylene-based chromophores functionalized with diaminotriazine head groups for hydrogen bonding.[38] With this method, one can obtain stable N-mers of any length. Measurement of the CD first spectral moment for each length, in principle, allows for the determination of the excitonic coupling between each pair of chromophores in the N-mer. Analysis of the experimental CD spectra can thus clarify the nature of extended couplings in helical assemblies, allowing for careful testing of dielectric screening effects as well as more sophisticated models that go beyond pairwise couplings.

Acknowledgment. This work is part of the research program of the "Stichting voor Fundamenteel Onderzoek der Materie (FOM)", which is financially supported by the Nederlandse Organisatie voor Wetenschappelijk Onderzoek (NWO). F.C.S. is supported by the NSF, Grant DMR No. 0906464. The authors thank Dr. David Beljonne and Dr. Stefan Meskers for providing us with the excitonic couplings and experimental data, respectively, and for valuable discussions.

Supporting Information Available: Extended overview of the model for helical MOPV4 aggregates. Derivation of the expression for the CD first spectral moment. Derivation of the rotational line strength in N-mers in the strong-disorder limit. This material is available free of charge via the Internet at http://pubs.acs.org.

References and Notes

(1) Fasman, G. D., Ed.; *Circular Dichroism and the Conformational Analysis of Biomolecules*; Plenum Press: New York, 1996.
(2) Lightner, D. A.; Gurst, J. E. *Organic Conformational Analysis and Stereochemistry from Circular Dichroism Spectroscopy*; Wiley-VCH: New York, 2000.
(3) Nakanishi, K.; Berova, N.; Woody, R. W., Eds.; *Circular Dichroism Principles and Applications*, 2nd ed.; Wiley-VCH: New York, 2000.
(4) Rodger, A.; Nordén, B. *Circular Dichroism and Linear Dichroism*; Oxford University Press Inc.: New York, 1997.
(5) Moerner, W. E. *J. Chem. Phys.* **2002**, *117*, 10925–10937.
(6) Spano, F. C. *J. Am. Chem. Soc.* **2009**, *131*, 4267–4278.
(7) Gottarelli, G.; Lena, S.; Masiero, S.; Pieraccini, S.; Spada, G. P. *Chirality* **2008**, *20*, 471–485.
(8) Lee, C. C.; Grenier, C.; Meijer, E. W.; Schenning, A. P. H. J. *Chem. Soc. Rev.* **2009**, *38*, 671–683.
(9) Amabilino, D. B.; Veciana, J. *Top. Curr. Chem.* **2006**, *265*, 253–302.
(10) Meijer, E. W.; Schenning, A. P. H. J. *Nature* **2002**, *419*, 353–354.
(11) Schenning, A. P. H. J.; Meijer, E. W. *Chem. Commun.* **2005**, *26*, 3245–3258.
(12) Schenning, A. P. H. J.; Jonkheijm, P.; Peeters, E.; Meijer, E. W. *J. Am. Chem. Soc.* **2001**, *123*, 409–416.
(13) Jonkheijm, P.; van der Schoot, P.; Schenning, A. P. H. J.; Meijer, E. W. *Science* **2006**, *313*, 80–83.
(14) Herz, L. M.; Daniel, C.; Silva, C.; Hoeben, F. J. M.; Schenning, A. P. H. J.; Meijer, E. W.; Friend, R. H.; Phillips, R. T. *Phys. Rev. B* **2003**, *68*, 045203.
(15) Beljonne, D.; Hennebicq, E.; Daniel, C.; Herz, L. M.; Silva, C.; Scholes, G. D.; Hoeben, F. J. M.; Jonkheijm, P.; Schenning, A. P. H. J.; Meskers, S. C. J.; Phillips, R. T.; Friend, R. H.; Meijer, E. W. *J. Phys. Chem. B* **2005**, *109*, 10594–10604.
(16) Prins, P.; Senthilkumar, K.; Grozema, F. C.; Jonkheijm, P.; Schenning, A. P. H. J.; Meijer, E. W.; Siebbeles, L. D. A. *J. Phys. Chem. B* **2005**, *109*, 18267–18274.
(17) Chang, M. H.; Hoeben, F. J. M.; Jonkheijm, P.; Schenning, A. P. H. J.; Meijer, E. W.; Silva, C.; Herz, L. M. *Chem. Phys. Lett.* **2006**, *418*, 196–201.
(18) Daniel, C.; Westenhoff, S.; Makereel, F.; Friend, R. H.; Beljonne, D.; Herz, L. M.; Silva, C. *J. Phys. Chem. C* **2007**, *111*, 19111–19119.
(19) Daniel, C.; Makereel, F.; Herz, L. M.; Hoeben, F. J. M.; Jonkheijm, P.; Schenning, A. P. H. J.; Meijer, E. W.; Silva, C. *J. Chem. Phys.* **2008**, *129*, 104701.
(20) Spano, F. C.; Meskers, S. C. J.; Hennebicq, E.; Beljonne, D. *J. Am. Chem. Soc.* **2007**, *129*, 7044–7054.
(21) Spano, F. C.; Meskers, S. C. J.; Hennebicq, E.; Beljonne, D. *J. Chem. Phys.* **2008**, *129*, 024704.
(22) van Dijk, L.; Kersten, S. P.; Jonkheijm, P.; van der Schoot, P.; Bobbert, P. A. *J. Phys. Chem. B* **2008**, *112*, 12386–12393.
(23) van Dijk, L.; Bobbert, P. A.; Spano, F. C. *J. Phys. Chem. B* **2009**, *113*, 9708–9717.
(24) Harada, N.; Chen, S. L.; Nakanishi, K. *J. Am. Chem. Soc.* **1975**, *97*, 5345–5352.
(25) Matile, S.; Berova, N.; Nakanishi, K.; Fleischhauer, J.; Woody, R. W. *J. Am. Chem. Soc.* **1996**, *118*, 5198–5206.

(26) Lewis, F. D.; Liu, X. Y.; Wu, Y. S.; Zuo, X. B. *J. Am. Chem. Soc.* **2003**, *125*, 12729–12731.

(27) Tsubaki, K.; Takaishi, K.; Tanaka, H.; Miura, M.; Kawabata, T. *Org. Lett.* **2006**, *8*, 2587–2590.

(28) Somsen, O. J. G.; van Grondelle, R.; van Amerongen, H. *Biophys. J.* **1996**, *71*, 1934–1951.

(29) Burin, A. L.; Armbruster, M. E.; Hariharan, M.; Lewis, F. D. *Proc. Natl. Acad. Sci. U.S.A.* **2009**, *106*, 989–994.

(30) Eisfeld, A.; Kniprath, R.; Briggs, J. S. *J. Chem. Phys.* **2007**, *126*, 104904–104916.

(31) Didraga, C.; Klugkist, J. A.; Knoester, J. *J. Phys. Chem. B* **2002**, *106*, 11474–11486.

(32) Holstein, T. *Ann. Phys.* **1959**, *8*, 325–342.

(33) Knapp, E. W. *Chem. Phys.* **1984**, *85*, 73–82.

(34) Cornil, J.; Beljonne, D.; Heller, C. M.; Campbell, I. H.; Laurich, B. K.; Smith, D. L.; Bradley, D. D. C.; Mullen, K.; Bredas, J. L. *Chem. Phys. Lett.* **1997**, *278*, 139–145.

(35) Philpott, M. R. *J. Chem. Phys.* **1971**, *55*, 2039–2054.

(36) Spano, F. C. *J. Chem. Phys.* **2002**, *116*, 5877–5891.

(37) Didraga, C.; Knoester, J. *J. Chem. Phys.* **2004**, *121*, 10687–10698.

(38) Janssen, P. G. A.; Jabbari-Farouji, S.; Surin, M.; Vila, X.; Gielen, J. C.; de Greef, T. F. A.; Vos, M. R. J.; Bomans, P. H. H.; Sommerdijk, N. A. J. M.; Christianen, P. C. M.; Leclère, P. E. L. G.; Lazzaroni, R.; van der Schoot, P. P. A. M.; Meijer, E. W.; Schenning, A. P. H. J. *J. Am. Chem. Soc.* **2009**, *131*, 1222–1231.

JP911081B